Mechanisms of Signal Transduction:

Epigen, the Last Ligand of ErbB Receptors, Reveals Intricate Relationships between Affinity and Mitogenicity

Bose S. Kochupurakkal, Daniel Harari, Ayelet Di-Segni, Galia Maik-Rachline, Ljuba Lyass, Gal Gur, Gabriele Kerber, Ami Citri, Sara Lavi, Raya Eilam, Vered Chalifa-Caspi, Zelig Eshhar, Eli Pikarsky, Ronit Pinkas-Kramarski, Sarah S. Bacus and Yosef Yarden

J. Biol. Chem. 2005, 280:8503-8512.
doi: 10.1074/jbc.M413919200 originally published online December 17, 2004

THE JOURNAL OF BIOLOGICAL CHEMISTRY
Vol. 280, No. 9, Issue of March 4, pp. 8503–8512, 2005
Printed in U.S.A.

Epigen, the Last Ligand of ErbB Receptors, Reveals Intricate Relationships between Affinity and Mitogenicity*

Received for publication, December 10, 2004
Published, JBC Papers in Press, December 17, 2004, DOI 10.1074/jbc.M413919200

Bose S. Kochupurakkal‡§, Daniel Harari‡§, Ayelet Di-Segni¶, Galia Maik-Rachline‡, Ljuba Lyass‖, Gal Gur‡, Gabriele Kerber‡, Ami Citri‡, Sara Lavi‡, Raya Eilam, Vered Chalifa-Caspi‡‡, Zelig Eshhar§§, Eli Pikarsky¶¶, Ronit Pinkas-Kramarski¶, Sarah S. Bacus‖, and Yosef Yarden‡‖‖**

*From the Departments of ‡Biological Regulation, **Veterinary Resources, and §§Immunology, The Weizmann Institute of Science, Rehovot 76100, Israel, the ¶Department of Neurobiochemistry, Tel-Aviv University, Ramat-Aviv 69978, Israel, ‖Targeted Molecular Diagnostics, Westmont, Illinois 60559, the ‡‡Life Science Department, Ben-Gurion University of the Negev, Beer Sheva 84105 Israel, and the ¶¶Department of Pathology, Hadassah University Hospital, Jerusalem 91120, Israel*

Four ErbB receptors and multiple growth factors sharing an epidermal growth factor (EGF) motif underlie transmembrane signaling by the ErbB family in development and cancer. Unlike other ErbB proteins, ErbB-2 binds no known EGF-like ligand. To address the existence of a direct ligand for ErbB-2, we applied algorithms based on genomic and cDNA structures to search sequence data bases. These searches reidentified all known EGF-like growth factors including Epigen (EPG), the least characterized ligand, but failed to identify novel factors. The precursor of EPG is a widely expressed transmembrane glycoprotein that undergoes cleavage at two sites to release a soluble EGF-like domain. A recombinant EPG cannot stimulate cells singly expressing ErbB-2, but it acts as a mitogen for cells expressing ErbB-1 and co-expressing ErbB-2 in combination with the other ErbBs. Interestingly, soluble EPG is more mitogenic than EGF, although its binding affinity is 100-fold lower. Our results attribute the anomalous mitogenic power of EPG to evasion of receptor-mediated depletion of ligand molecules, as well as to inefficient receptor ubiquitylation and down-regulation. In conclusion, EPG might represent the last EGF-like growth factor and define a category of low affinity ligands, whose bioactivity differs from the more extensively studied high affinity ligands.

Growth factors play important roles in developmental cell lineage determination and in tissue remodeling throughout adulthood. One of the most extensively studied families of growth factors comprises polypeptides sharing an epidermal growth factor (EGF)[1] motif (reviewed in Ref. 1). This highly conserved motif, which includes six canonical cysteines, binds to a family of four cell surface receptors, called ErbB (or HER) proteins. The extracellular domain of each ErbB protein displays binding specificity to several EGF-like ligands, which activate the intracellular tyrosine kinase. Notably, ErbB-3 binds several types of neuregulins, but its tyrosine kinase domain is catalytically inactive (2). Conversely, ErbB-2 binds with no known ligand directly but is transactivated through heterodimerization with other ErbBs (3).

Interestingly, ErbB-2 is widely expressed in a dynamic and heterogeneous manner. An example is provided by human tumors of mammary and ovarian origins; because of gene amplification, ErbB-2 is overexpressed in a subset of relatively aggressive tumors (4). The apparent absence of a *bone fide* ligand for ErbB-2 is also relevant to another route of ErbB-mediated oncogenesis, namely increased production of a growth factor where autocrine ligand secretion drives proliferation of various cancers (reviewed in Ref. 5). Because ErbB-2 is a widely expressed oncoprotein and antibodies directed at this surface antigen can prolong survival of breast cancer patients (6), it is crucial to examine the contention that ErbB-2 functions as a ligand-less co-receptor, which enhances and prolongs signaling by autocrine or stroma-derived EGF-like ligands (reviewed in Ref. 7).

The ErbB family presents another open question that relates to the multiplicity of EGF-like ligands sharing specificity to the same receptor (reviewed by Ref. 8). Thus, along with EGF and the transforming growth factor α (TGFα), ErbB-1 binds the heparin-binding EGF-like growth factor (HB-EGF), Betacellulin, Amphiregulin (*AR*), Epiregulin, and Epigen (9). Likewise, several ligands that bind ErbB-4 also bind ErbB-1, with the exception of NRG-3 and NRG-4, which bind ErbB-4 exclusively. Genetic manipulation of EGF-like ligands in mammals assigned partially overlapping but distinct functions to individual growth factors, in processes as diverse as mammary, cardiac and intestinal development, and wound healing (see for example Ref. 10). These and other lines of evidence imply that ligand multiplicity reflects functional features unique to each EGF-like growth factor.

The present study addressed the multiplicity of EGF-like molecules and the possibility that mammalian genomes encode a yet uncharacterized ligand for ErbB-2. By designing a genome-wide screen that can identify ErbB ligands on the basis of their intron-exon organization, we reidentified all known ligands of ErbB proteins but found no novel molecule that can potentially qualify as an ErbB-2 ligand. Concentrating on the least characterized member of the EGF family, namely Epigen (EPG), we highlight several biochemical and physiological at-

* This work was supported by The Prostate Cancer Foundation and by NCI, National Institutes of Health Grant CA72981. The costs of publication of this article were defrayed in part by the payment of page charges. This article must therefore be hereby marked "*advertisement*" in accordance with 18 U.S.C. Section 1734 solely to indicate this fact.

§ Both authors contributed equally to this work.

‖‖ Incumbent of the Harold and Zelda Goldenberg Professorial Chair. To whom correspondence should be addressed: Dept. of Biological Regulation, The Weizmann Institute of Science, 1 Hertzl St., Rehovot 76100, Israel. Tel.: 972-8-9343974; Fax: 972-8-9342488; E-mail: yosef.yarden@weizmann.ac.il.

[1] The abbreviations used are: EGF, epidermal growth factor; CHO, Chinese hamster ovary; EPG, Epigen; EPR, Epiregulin; IL-3, interleukin-3; NRG, Neuregulin; TGFα, transforming growth factor α; HB, heparin-binding; HA, hemagglutinin; EndoH, endoglycosidase H; Tricine, *N*-[2-hydroxy-1,1-bis(hydroxymethyl)ethyl]glycine; PNGaseF, peptide *N*-glycosidase F; E3, ubiquitin-protein isopeptide ligase.

tributes that distinguish low affinity ligands from the extensively characterized high affinity family members.

MATERIALS AND METHODS

Bioinformatics and Phylogenetics—The approximate exon-intron boundary for each EGF-like gene was determined (using tblastn) by comparison of the protein sequence for each gene with the corresponding genomic locus. For the purpose of the data base searches performed herein, the EGF domain was defined as that encoding the six invariant cysteine residues of the domain and the additional five flanking amino acids both N- and C-terminally to cysteine 1 and cysteine 6, respectively. Two separate multiple alignments were generated for sequences encoding Exon-1 and Exon-2, which were then compiled into two independent profiles (Profilemake; GCG10). The profiles were used as criteria for a stepwise Smith-Waterman-based search of human genomic data (Biocellerator device, Compugen, Israel; HTGS and NR data bases). The first 2000 hits from the Exon-1 profile search were saved and recompiled into a new, miniature data base using PERL script. These 2000 sequences were then scanned, this time using the Exon-2 profile, to identify EGF-like ligands. The human Epigen-Epiregulin genomic locus was extracted from a data base provided by Celera Genomics. Their localization to chromosome 4q21.21 was assigned with the aid of NCBI MapView (version 34). Phylogenetic data were generated with the aid of ClustalX (version 1.81; default settings) and visualized with a modification of an output generated from TREEVIEW (11).

Expression of Pro-Epigen in Mammalian Cells—The coding sequence of pro-EPG was amplified using PCR from an IMAGE clone (GenBank™; BU540655) and cloned into pIRES-puro vector (12), with or without a C-terminal HA tag. The plasmid was transfected into CHO cells, and stable clones were selected with 10 μg/ml puromycin. Immunoprecipitates of anti-HA (Roche Applied Science) and anti-EPG antibodies were equilibrated with 50 mM citrate (pH 5.5) or saline for deglycosylation using endoglycosidase H (EndoH) or peptide *N*-glycosidase F, respectively. Deglycosylation was performed at 37 °C for 2 h. The proteins were separated on a 16.5% Tricine gel and transferred to an Immobilon-P membrane (Millipore, Bedford, MA). To biotinylate cell surface proteins, the cell monolayers were washed with saline and incubated with biotin-*N*-hydroxysuccinimidyl ester (Pierce) for 1 h on ice. Excess biotin was quenched using 100 mM glycine in saline, and the cells were washed extensively and incubated at 37 °C.

Expression and Purification of Recombinant Growth Factors—The EGF-like domain, including five residues N-terminal to cysteine 1 and five and eight residues C-terminal to cysteine 6 of human NRG-β1 and human EPG, respectively, was cloned into the pET32b vector and expressed as C-terminal thioredoxin fusion proteins with the Factor Xa cleavage site adjacent to the N-terminal residue of the EGF-like domain. The proteins were expressed in *Escherichia coli* (BL21) using standard procedures. Expressed proteins were first purified on a nickel-nitrilotriacetic acid column, cleaved using Factor-Xa (New England Biolabs, Beverly, MA), and then purified on a Superdex-30 (Amersham Biosciences) column.

Generation and Affinity Purification of an Anti-EPG Antibody—New Zealand rabbits were immunized with a purified EGF-like domain of EPG (0.1 mg). For affinity purification, a recombinant EPG fusion protein was immobilized on cyanogen bromide-activated Sepharose 4B (Amersham Biosciences) according to the manufacturer's protocol. The serum was diluted 10-fold using column buffer (Tris-HCl, pH 8.0, 250 mM NaCl) and passed through the column. The column was then washed extensively, and bound proteins were eluted using 100 mM glycine-HCl (pH 2.5).

Cell Proliferation and Stimulation Assays—A previously described method (13) has been used with the following modifications: 5×10^4 32D cells were plated in triplicate in a 96-well plate and treated with different concentrations of ligand or with a fixed ligand concentration (100 ng/ml) for different time intervals. In experiments with extended periods of treatment, the cells were plated at a density of 1000 cells/well of a 96-well plate. The cells were harvested at each time point and incubated with 3-(4,5-dimethylthiazol-2-yl)-2,5-diphenyltetrazolium bromide (0.1 mg/ml) for 2 h. Thereafter, the cells were extracted with acidified 2-propanol, and the optical density was measured at 570 nM with a reference 650 nM filter. For receptor stimulation, 32D cells were washed extensively in medium devoid of interleukin-3 (IL-3) and divided equally. The cells were then stimulated with various ligands for different periods of time, collected by centrifugation, and lysed in lysis buffer, and equal amounts of lysate were separated using gel electrophoresis. Separated proteins were then transferred onto nitrocellulose membranes and probed with specific antibodies.

Ligand Binding Assays—Ligands were radiolabeled using Iodogen (Pierce) following the manufacturer's protocol. Cells grown in 48-well plates were washed with ice-cold binding buffer (Dulbecco's modified Eagle's medium containing 20 mM HEPES, pH 7.5, and 0.1% albumin) and incubated on ice for 3 h with different ligand concentrations in duplicates. Thereafter, media were aspirated, cells were washed and extracted in 0.1% sodium dodecylsulfate and 0.1 N NaOH, and cell-associated radioactivity was determined.

Ligand Degradation Assay—Cos-7 cells were equally plated in a 48-well plate, and the experiment was performed in duplicates. Nonspecific binding was determined with 100-fold excess unlabeled EGF. The cells were washed, equilibrated with binding buffer at 37 °C, and incubated with radiolabeled ligands at 37 °C. After incubation, the medium was collected, and intact ligand in the medium was precipitated using trichloroacetic acid. The cells were washed once with warm binding buffer, and this was added to the medium fraction. The cells were then transferred to ice and incubated with cold acid wash buffer (50 mM glycine-HCl, pH 3.0, 100 mM NaCl, 2 mg/ml polyvinylpyrrolidone). The wash buffer was collected, and radioactivity associated with this sample was considered as the surface-bound ligand. Lysates of the cells were also prepared. The sum of radioactivity obtained in the acid-precipitable and acid wash fractions was considered as intact extracellular ligand.

Sensitivity of Ligand Binding to pH—A431 cells were plated equally in 48-well plates, and the experiment was performed in duplicates. After 24 h, the cells were moved to ice and equilibrated with 50 mM phosphate buffers at different pH levels (7.5–6.0) containing 100 mM NaCl and 0.1% albumin. The equilibrated cells were then incubated for 2 h on ice with ligand-containing solutions buffered at various pH levels. At the end of the incubation, the cells were washed twice with buffers at the respective pH level. The cells were lysed, and associated radioactivity was measured using a γ-counter.

Receptor Ubiquitylation Assay—Cos-7 cells were transiently transfected with the indicated plasmids using Lipofectamine (Invitrogen). Forty-eight hours later, the cells were stimulated with EGF or EPG for 10 min. ErbB-1 was immunoprecipitated from cell lysates, or the lysate was directly resolved by electrophoresis. Separated proteins were then transferred onto a nitrocellulose membrane and probed with antibodies to HA (Roche Applied Science), ErbB-1 (Santa Cruz Biotechnology, Santa Cruz, CA), or c-Cbl (Santa Cruz).

Receptor Down-regulation Assay—Cos-7 cells were transfected with plasmids encoding ErbB-1, along with a c-Cbl plasmid as indicated. Twenty-four hours later, the cells were divided into 6-well plates, and after another 24 h the cells were stimulated with various ligands at 37 °C. At the end of each time interval, the plates were placed on ice, surface-bound ligand was stripped using acid wash buffer (150 mM acetic acid and 150 mM NaCl), and the cells were incubated for 2 h with ^{125}I-EGF (5 ng/ml) in binding buffer. Following incubation, the cells were washed using binding buffer, and cell-associated radioactivity was determined.

Immunohistochemistry Using Anti-EPG Antibodies—Murine tissues were isolated, frozen in powdered dry ice, and embedded in paraffin. Staining was performed on 10-μm thick paraffin sections after an antigen retrieval procedure using 10 mM citric acid (pH 6.0). Tissue sections were first blocked using normal serum and then incubated with the anti-EPG antibody (0.5 μg/ml) or anti-TGFα (BioTope). Visualization was achieved using the Vectastain ABC system (Vectorlabs, Burlingham, CA) or donkey anti-rabbit and anti-rat fluorescent antibodies (Jackson ImmunoResearch, West Grove, PA). Human tissue sections were stained with the anti-EPG antibody using a similar protocol.

PCR Analysis of EPG Expression—Prostate cancer xenografts were grown in castrated (androgen-independent) and noncastrated (androgen-dependent) nude mice, as described (14). Total RNA was isolated from 0.1 mg of each tissue using TRIzol (Sigma). Primers for PCR were selected within the coding region of EPG using the web interface of the Primer 3 software (MIT.EDU). The reverse transcriptase reaction with a sample of total RNA was performed using Superscript (Invitrogen), and PCRs were performed using BioTaq (Bioline, London, UK) for 30 cycles. A second round of PCR was performed to increase the amount of product, and the samples were divided into two. One part was left untreated, and the other was digested with NdeI.

Cell Differentiation and Aortic Ring Assays—Differentiation of mammary cells has been described before (15). PC12 cells stably expressing ErbB-4 (16) were plated in 24-well, collagen-coated plates and treated with the indicated ligands (100 ng/ml) for 7 days. Normal human prostate epithelial cells, RWPE-1, were plated on growth factor-depleted Matrigel at a density of 1000 cells/well in a 96-well plate. The cells were incubated with KSFM medium (Invitrogen) (17) containing

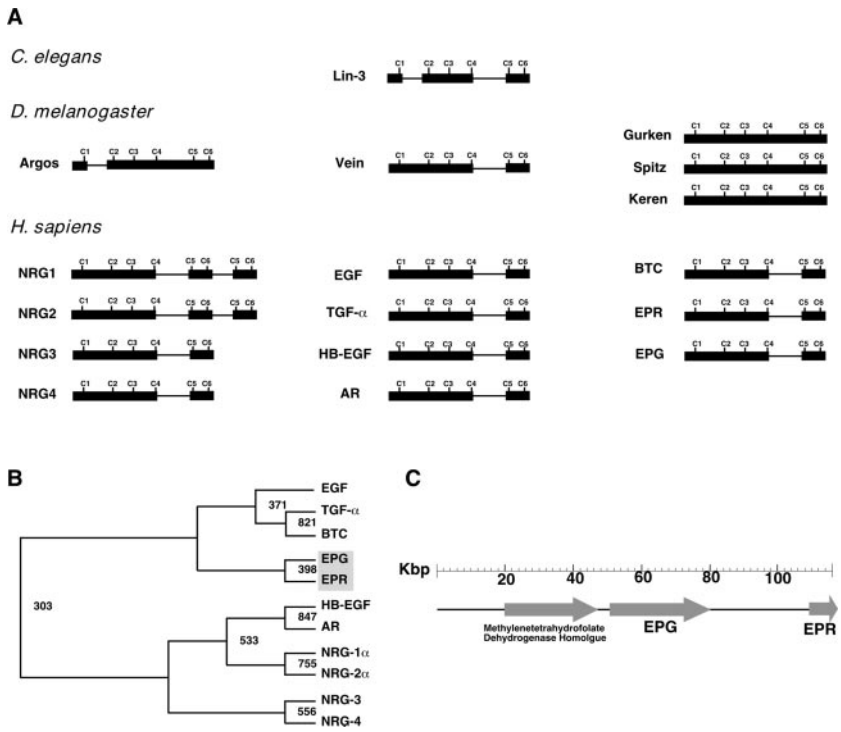

FIG. 1. **Chromosomal organization and structural features of EGF-like molecules.** *A*, the intron-exon structures of the EGF-like domains of invertebrate (*C. elegans* and *Drosophila melanogaster*) and mammalian (*Homo sapiens*) ErbB ligands are schematically presented. The six canonical cysteine (*C*) residues of the EGF motif are marked and numbered. *AR*, Amphiregulin; *BTC*, Betacellulin. *B*, an unrooted phylogenetic tree showing the evolutionary relatedness of the various human EGF-like ligands. The bootstrap values (of 1000 trials) are indicated, and the Epigen/Epiregulin pair is highlighted. *C*, co-localization of the *epigen* and *epiregulin* genes to human chromosome 4q21. Only the 5′ portion of the *epiregulin* gene is presented, along with its transcriptional orientation.

growth factors at 100 ng/ml for 5 days, and the medium was replenished after 3 days. Aortas from 6–10-week-old mice were isolated, cleaned of surrounding tissue, and washed with saline. Each aorta was cut into 1-mm-thick rings and embedded in collagen (isolated from rat tail). The rings were then incubated in medium, either with or without growth factors (at 100 ng/ml). The medium was changed every 3 days, and the rings were monitored for up to 14 days. To visualize microvessels, the rings were fixed overnight using 4% formaldehyde in saline, stained for 4 h with a solution containing 0.02% crystal violet in 50% ethanol, and subsequently destained.

RESULTS

A Genome-wide Screen Reidentified All Known EGF-like Molecules, Including the Most Recent Addition, Epigen—Previously we have reported the discovery of NRG-4 using a bioinformatics approach (18), where the search criteria were based on the six conserved cysteine residues of the EGF-like domain. Repeated searches of the expanded expressed sequence tag data base detected no novel ligands, which led us to examine alternative strategies. Analyses of the genomic structure of the known ErbB ligands revealed that the EGF-like domain of all the mammalian ligands are encoded by two exons (defined here as Exon-1 and Exon-2), where Exon-1 encodes four of the N-terminal cysteine residues, and Exon-2 encodes cysteines 5 and 6 (Fig. 1*A*). *NRG1* and *NRG2* genes harbor a supplementary Exon-2, and through alternative splicing, Exon-1 is fused to either the first or the second Exon-2, thereby generating the α or β isoforms. Interestingly, the EGF-like domain of Lin-3, the single EGF-like growth factor in *Caenorhabditis elegans*, is encoded by three exons, but the five corresponding genes of *Drosophila* display three different genomic patterns in the EGF-like domains, including one (*vein*) that resembles the mammalian pattern (Fig. 1*A*).

The conserved genomic organization of the different mammalian ErbB ligands provided a means in which a stepwise Smith-Waterman-based search could be employed to screen for new EGF-like ligands from genomic data. Unlike gapped BLAST searches, Smith-Waterman-based searches are unable to accommodate large gaps (*e.g.* intron sequences) when performing sequence alignments. Hence, the search procedure was performed as follows. First, two separate multiple sequence alignments were generated corresponding to the segments of the EGF-like domains encoded by Exon-1 and Exon-2 for all known ligands. These alignments were then converted into two sequence profiles. The profile of protein sequences encoded by Exon-1 was then used as a bait to perform a Smith-Waterman-based profile search against genomic sequence data (detailed under "Materials and Methods"). The first 2000 hits from this search were recompiled into a miniature data base. This data base was then searched once again using the sequence profile generated from Exon-2. All hits harboring both Exon-1- and Exon-2-encoding sequences were thus identified. Using this methodology, we detected all of the ErbB ligands for which genomic sequences are available (all ligands but Betacellulin), including the most recent addition, namely Epigen (9). To test the power of the genomic search, we created a series of sequence profiles, each lacking a single ErbB ligand and used them to rescreen the genomic and expressed sequence tag data bases. In each case, the missing ligand was reidentified from the genomic data, demonstrating that the search strategy is robust. Hence, we concluded that the combined expressed sequence tag and genomic search strategies are exhaustive, with no novel ligands being identified.

Alignment of the EGF-like motifs of all human ErbB ligands indicated that EPG is most similar to EPG. A phylogeny analysis clustered five ligands of ErbB-1 and revealed an Epigen-Epiregulin relationship (Fig. 1*B*). Because of the small length of the EGF domain and the high disparity of sequence identity between different members of the family, the significance of the Epigen-Epiregulin clustering is not particularly high (a bootstrap value of 398 of 1000 trials). Nevertheless, in support of relatedness, EPG and EPR co-localize to the same genomic locus, at chromosomal position 4q21, and their open reading frames are separated by a mere 25 kilobase pairs (Fig. 1*C*). Similarly, this genomic linkage is evident in mice (data not shown), demonstrating that the Epiregulin-Epigen microchromosomal duplication took place in mammals before the evolutionary diversion of primates and rodents.

Pro-Epigen Is a Transmembrane Glycoprotein Processed at Two Proteolytic Sites—Analysis of the primary sequence of

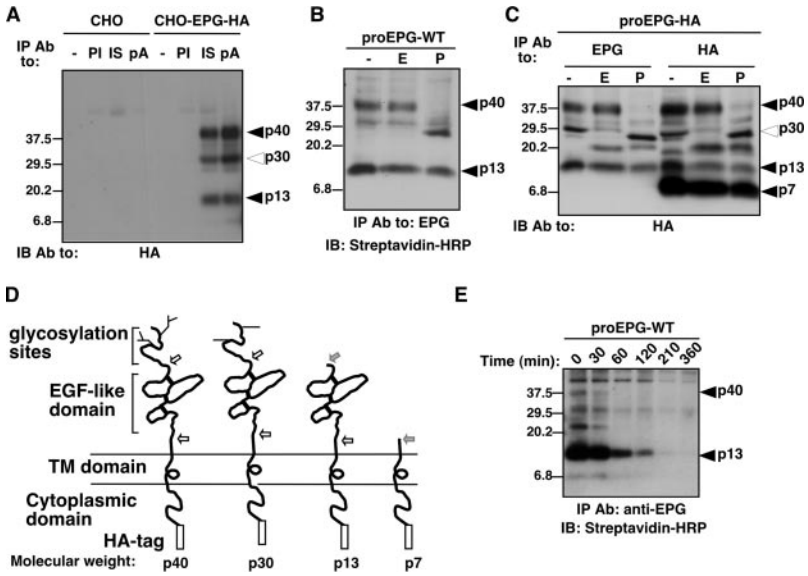

FIG. 2. **Pro-Epigen is a transmembrane glycoprotein processed at two proteolytic sites.** *A*, full-length human EPG fused to a HA peptide tag was stably expressed in CHO cells. Untransfected CHO cells were used as control. Whole cell extracts were subjected to immunoprecipitation (*IP*) and immunoblotting (*IB*). The following antibodies were used for immunoprecipitation: no serum control (−), a preimmune serum (*PI*), an immune rabbit serum to EPG (*IS*), and an affinity-purified antibody (*pA*). *Arrowheads* mark the locations of pro-EPG forms. *Ab*, antibody. *B*, CHO cells stably expressing untagged pro-EPG (*WT*) were incubated on ice for 1 h with biotin-*N*-hydroxysuccinimidyl ester to label surface proteins. Excess biotin was quenched, and the lysates were prepared. The proteins were immunoprecipitated using anti-EPG antibodies, and the immunoprecipitates were left untreated (−), treated with EndoH (*E*), or treated with PNGaseF (*P*). Thereafter, the proteins were electrophoretically separated and transferred onto a membrane, and the membrane was probed using streptavidin-horseradish peroxidase. *C*, HA-tagged pro-EPG expressed in CHO cells was immunoprecipitated using the indicated antibodies, and the immunoprecipitates were treated as in *B* and subjected to immunoblotting with an anti-HA antibody. *D*, a schematic view of pro-EPG and the locations of putative proteolytic cleavage sites (*arrows*). Cysteine bridges within the EGF-like domain are indicated. *E*, the surface of pro-EPG-expressing cells was biotinylated, and the cell extracts were analyzed as in *B*, except that following quenching of active biotin, the cells were incubated at 37 °C for the indicated time intervals, prior to immunoprecipitation.

pro-EPG predicts a type-1 transmembrane protein (9), but no data are available on glycosylation, proteolytic processing, or association with the plasma membrane. To address these issues, we stably expressed in CHO cells full-length pro-EPG, with and without a HA peptide tag at the C terminus. In addition, we immunized rabbits with recombinant EPG expressed in bacteria (rEPG, see below) and affinity-purified the antiserum. The immune serum and the purified antibody specifically recognized three proteins (p40, p30, and p13) in pro-EPG-expressing cells (Fig. 2*A*). Labeling of the surface of pro-EPG-expressing CHO cells with biotin detected p40 and p13 (Fig. 2*B*), indicating that p30 is an intracellular protein and confirming delivery of pro-EPG to the plasma membrane. To further prove that p40 is expressed at the cell surface, we tested the acquisition of resistance to EndoH, which parallels translocation of EndoH-sensitive high mannose precursors from the endoplasmic reticulum to the Golgi apparatus. Separately, immunoprecipitates of EPG were treated with peptide *N*-glycosidase F (PNGaseF), an enzyme that cleaves all *N*-linked glycans but core fucosylated chains. Biotin labeled pro-EPG (p40) was susceptible to PNGaseF but resistant to EndoH (Fig. 2*B*), indicating that modifications of asparagine-linked oligosaccharides of pro-EPG is completed in the Golgi, prior to delivery to the cell surface.

Unlike p40, p13 displayed resistance to both EndoH and PNGaseF, and p30 was resistant to EndoH but sensitive to PNGaseF (Fig. 2, *B* and *C*). In addition to p13, p30, and p40, anti-HA antibodies detected a fourth protein, p7, which displayed resistance to both enzymes. On the basis of these results, and the presence of two predicted asparagine-based glycosylation sites, we inferred that pro-EPG carries an N-terminal *N*-glycosylation domain and two putative cleavage sites (Fig. 2*D*). To test this model, we surface-labeled pro-EPG-expressing cells with biotin, quenched reactive biotin, and chased cells in fresh medium. The most prominently labeled species was p13, suggesting that cleavage at the N-terminal site of pro-EPG precedes proteolysis at the membrane-flanking site (probably an Ala^{103}-Val motif, similar to other EGF-like ligands; Fig. 2*E*). In summary, following insertion in the plasma membrane, the precursor of EPG undergoes two proteolytic cleavage events; a relatively rapid event releases the glycosylated domain, and a subsequent event clips within the short segment connecting the EGF-like domain with the transmembrane helix.

Epigen Cannot Stimulate ErbB-2 in Isolation—EPG is the least characterized EGF-like ligand (9), and its interaction with ErbB-2 has not been investigated. Therefore, we expressed EPG, as well as NRG-1β for control, as thioredoxin fusion proteins in bacteria, cleaved the products to remove thioredoxin, and purified the recombinant growth factors to homogeneity. Radiolabeling of rEPG confirmed absence of trace impurities (Fig. 3*A*), and mass spectrometry yielded a molecular mass consistent with oxidation of all cysteines. Next, we tested whether EPG could activate ErbB-2 in the absence of other members of the ErbB family. The D2 derivative of the IL-3-dependent 32D myeloid cell line, stably expressing human ErbB-2 on an ErbB-null background, was used (19). Although IL-3 supported robust cell proliferation, treatment of D2 cells with rEPG in the absence of IL-3 resulted in growth arrest and partial cell death (Fig. 3*B*). These results indicate that EPG, like its closest homologue, EPR (20), and in fact all other members of the EGF family, is unable to stimulate ErbB-2 in the absence of other ErbBs.

Epigen Is a Potent Activator of ErbB-1 Despite Low Binding Affinity—Next we analyzed the activity of EPG toward the other ErbB receptors. We used derivatives of the 32D cell line expressing ErbB-1 (D1), ErbB-3 (D3), or ErbB-4 (D4), either singly or in combination with ErbB-2 (D12, D23, and D24).

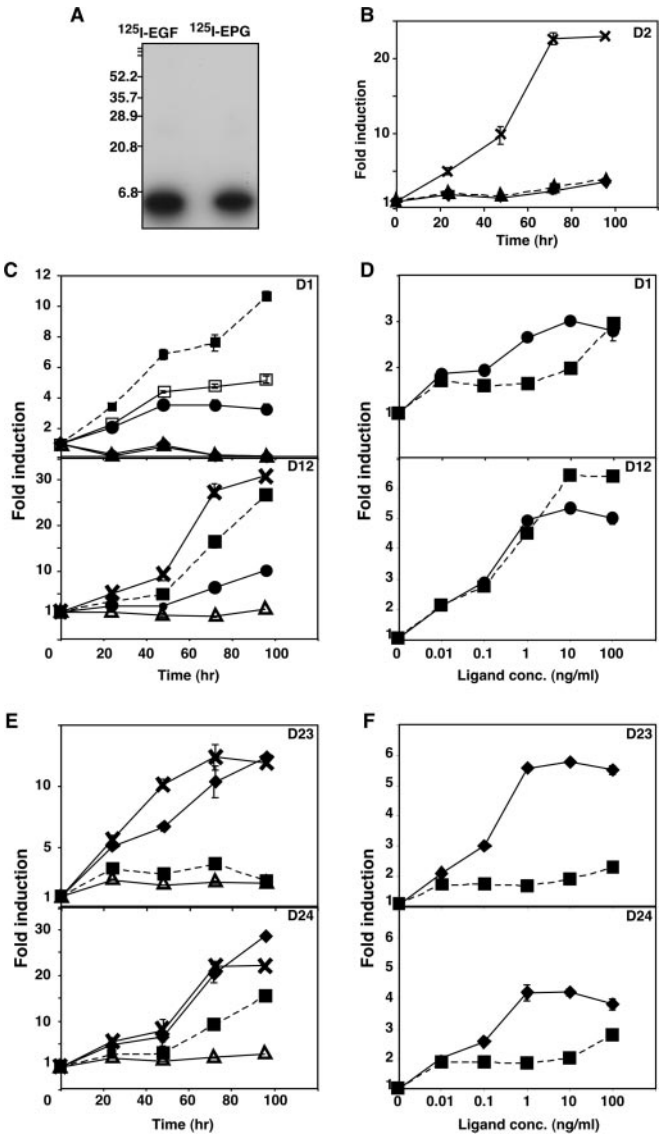

FIG. 3. **Epigen cannot directly stimulate ErbB-2 and it acts as a potent activator of ErbB-1.** *A,* recombinant EPG was purified from bacteria using nickel-nitrilotriacetic acid and Superdex 30 columns. Radiolabeled rEPG, as well as a radioactive EGF, were separated on a 16% Tricine gel. The resulting autoradiogram is shown, along with the locations of molecular mass markers (in kDa). *B–F*, 32D myeloid cells stably expressing ErbB-2 (*B*; D2 cells), ErbB-1 alone (D1) or co-expressing ErbB-2 along with ErbB-1 (D12 cells; *C* and *D*), and cells co-expressing ErbB-2 along with either ErbB-3 (D23), or ErbB-4 (D24; *E* and *F*) were grown in the presence of IL-3 (*crosses*), EPG (*filled squares* and a *dashed line*), TGFα (*open squares*), EGF (*filled circles*), NRG-1β (*filled diamonds*), or solvent (*open triangles*). The 3-(4,5-dimethylthiazol-2-yl)-2,5-diphenyltetrazolium bromide cell proliferation assay was performed four times over 4 days or with increasing ligand concentrations. The results (mean ± S.D.) are plotted as fold induction relative to the initial level.

When D1 cells were treated with EGF, TGFα, and EPG over 4 days, EPG was found to be the most potent mitogen in comparison with the other ligands (Fig. 3*C*). Under similar experimental conditions neither D3 nor D4 cells displayed significant responses to EPG (data not shown). In line with the notion that ErbB-2 enhances signaling by the other ErbB receptors, the induction of proliferation observed in EPG-treated D12 cells was higher than in D1 cells (Fig. 3, *C* and *D*), and both D23 and D24 cells showed increases in cell proliferation, as reflected in both kinetics and dose curves (Fig. 3, *E* and *F*). Stimulation of the 32D cell lines with EGF or NRG-1β induced robust receptor phosphorylation, whereas the activity of EPG was relatively weak (Fig. 4, *A* and *B*, and data not shown). However, in the case of D1 and D12 cells, where EPG induces relatively potent mitogenic responses, the weak EPG-induced receptor phosphorylation was sustained up to 45 min, and extracellular signal-regulated kinase/mitogen-activated protein kinase signals were almost comparable with those induced by EGF (Fig. 4, *A* and *B*).

To understand what bearing the binding affinity of EPG has on its relatively high mitogenicity, ligand displacement analyses were performed. Unexpectedly, displacement of a radiolabeled EGF by EPG indicated an ~100-fold difference in binding affinity, in favor of EGF (Fig. 4*C*, *left panel*). The reciprocal assay, which used a radiolabeled EPG and an unlabeled EGF, corroborated this finding (Fig. 4*C*, *right panel*). Further, the bi-sigmoidal curve observed for the displacement of EPG by EGF suggested the existence of two receptor populations. The very low binding affinity of EPG is surprising in light of its biological potency, which resembles the case of the sibling of Epigen, namely EPR (20, 21).

In summary, EPG is a low affinity/broad specificity growth factor that effectively activates ErbB-1. Surprisingly, EPG is a more potent mitogen than EGF, especially at high (>10 ng/ml) ligand concentrations where EPG activates a subset of ErbB-1 molecules on the cell surface. Further, EPG can activate ErbB-4 and ErbB-3 when these receptors are co-expressed with ErbB-2.

The Anomalous Mitogenic Potential of EPG Is Attributable to Evasion of Desensitization Mechanisms—To understand the superior mitogenic power of EPG, as compared with other ErbB-1 ligands whose binding affinities are significantly higher (Fig. 3*C*), we examined dose-response curves obtained with D1 cells over a period of 6 days (Fig. 5*A*). As expected, bell-shaped curves were obtained when EGF and TGFα were tested, but in contrast monotonic dose-response curves were observed with EPG at all of the time widows we tested (Fig. 5*A*). Cell proliferation was only observed at ligand concentrations above 0.1 ng/ml, and the maximal response obtained for each ligand, namely EGF (1 ng/ml), TGFα (10 ng/ml), and EPG (100 ng/ml), corresponded to the relative binding affinities. Because the dose-response curve of EPG lacked a descending phase, which is attributed to desensitization process like ligand consumption and receptor down-regulation (Ref. 22 and references therein), we compared the effectiveness of desensitization of EPG signals with that of EGF and TGFα.

Receptor-mediated endocytosis is considered the major desensitization process of EGF-like growth factors, because it robustly removes ligands from the extracellular space and simultaneously targets cell surface receptors to intracellular degradation (reviewed in Ref. 23). The ligand degradation assay presented in Fig. 5*B* follows the rate of ligand clearance from the extracellular milieu. When Cos-7 cells were stimulated with EGF, TGFα, and EPG, we found that EGF was consumed to a much larger extent than EPG and TGFα. Because TGFα recycles back to the cell surface because of dissociation of ligand-receptor complexes in the acidic endosomal compartment (24), we tested the pH dependence of the interaction between EPG and EGFR/ErbB-1 (Fig. 5*C*). A431 cells were incubated with EGF, TGFα, and EPG in buffers at pH ranging from 6.0 to 7.5. A drop in pH from 7.5 to 7.2 caused dissociation of ~70% of bound TGFα and ~50% of bound EPG, whereas only 25% of bound EGF dissociated from the receptor. Thus, EPG partly shares with TFGα sensitivity to low pH. The acid-sensitive binding of TFGα is attributable to histidine residues embedded in the pocket of a hydrophobic receptor with solvent-accessible surfaces (25), and our homology modeling suggests that histi-

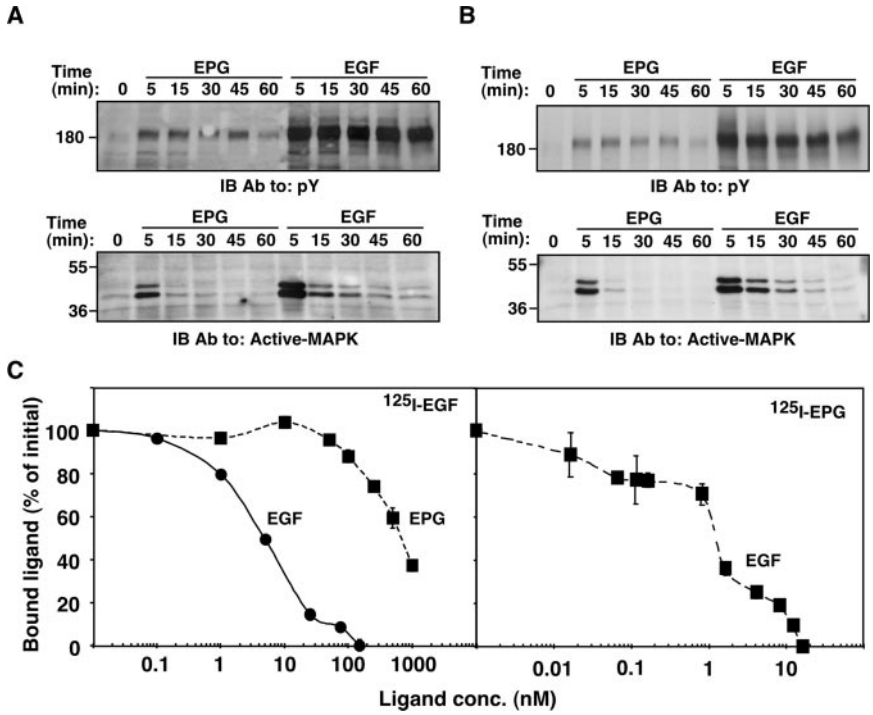

FIG. 4. **Epigen is a low affinity/broad-specificity ligand that weakly stimulates receptor phosphorylation.** *A* and *B*, derivatives of myeloid cells, D1 (*A*) and D12 (*B*) cells, were washed thoroughly and stimulated with EGF or EPG (each at 100 ng/ml) for the indicated periods of time. Equal amounts of whole cell extracts were then immunoblotted (*IB*) using anti-phosphotyrosine (*pY*) and anti-phospho-extracellular signal-regulated kinase/mitogen-activated protein kinase (*MAPK*) antibodies. *C*, CHO cells (*left panel*) and Cos-7 cells (*right panel*) stably or transiently overexpressing ErbB-1, respectively, were used for ligand displacement assays. The cells in a 48-well plate were incubated for 3 h on ice with radiolabeled EGF (1 nM) or EPG (100 nM) in the absence or presence of increasing concentrations of the competing unlabeled ligand, as indicated. The cells were later washed and lysed, and associated radioactivity was determined. The extent of ligand displacement (mean ± range of duplicates) was plotted with respect to binding in the absence of an unlabeled ligand. *Ab*, antibody.

dines 23 and 43 of EPG are responsible for acid sensitivity (data not shown).

Like EPG, ErbB ligands encoded by poxviruses display lower binding affinity relative to their mammalian counterparts, but their biological activities are superior because of ineffective endocytosis of ligand-receptor complexes (26). A master regulator of ErbB-1 endocytosis is c-Cbl, an E3 ubiquitin ligase that sorts active receptors to degradation in lysosomes by tagging them with ubiquitin (reviewed in Ref. 27). To test the prediction that Cbl-mediated ubiquitylation ineffectively sorts EPG-activated receptors relative to EGF-bound ErbB-1 molecules, we used Cos-7 cells. The cells were transfected with a c-Cbl plasmid, or a control empty vector, along with vectors encoding ErbB-1 and HA-tagged ubiquitin, and receptor ubiquitylation was monitored following stimulation for 10 min with either EPG or EGF. As has previously been reported (28), when overexpressed, ectopic c-Cbl enhanced ubiquitylation of EGF-stimulated ErbB-1 molecules and accelerated their degradation (Fig. 5*D*). In comparison with EGF, EPG induced significantly weaker ubiquitylation and degradation of ErbB-1.

To further confirm that EPG-stimulated receptors are inefficiently targeted for degradation, we assayed receptor down-regulation (Fig. 5*E*). Cos-7 cells were co-transfected with plasmids encoding ErbB-1 and either an empty vector (Fig. 5*E*, *upper panel*) or a c-Cbl plasmid (Fig. 5*E*, *lower panel*). Thereafter, the cells were stimulated with EGF, TGFα, or EPG for increasing time intervals, and loss of cell surface receptors was monitored using a radiolabeled EGF. EGF stimulation resulted in the loss of more than half of the cell surface receptors within 150 min, and an additional loss of receptor was observed in c-Cbl overexpressing cells. When stimulated with TGFα, ~35% of the receptors were lost from the cell surface, and overexpression of c-Cbl had no effect. Stimulation by EPG resulted in the loss of only about 20% of the receptors from the cell surface, and modest effects were observed in cells overexpressing c-Cbl.

In conclusion, the anomalous mitogenic potential of EPG is due primarily to low affinity binding to the cell surface sites (Fig. 4*C*), which exerts a dual action. First, it dictates rapid ligand dissociation, whose effect is augmented by sensitivity to low pH and consequent recycling of EPG to the cell surface (Fig. 5*C*). Hence, the rate of EPG depletion is slower than the rate displayed by EGF and TGFα (Fig. 5*B*), which enhances and prolongs mitogenic signals. On the other hand, EPG induces only limited receptor phosphorylation relative to a high affinity ligand like EGF (Fig. 4*A*). The outcome is inefficient recruitment of c-Cbl, relatively weak ubiquitylation (Fig. 5*D*) and inefficient EPG-induced receptor down-regulation (Fig. 5*E*) and degradation (Fig. 5*D*, *middle panel*).

Epigen Is Widely Expressed in Mouse Tissues and Human Tumors—Northern blot analysis detected EPG mRNA in multiple mouse tissues (9), but no data are available on protein expression. To decipher what cell types express EPG, we analyzed embryonic day 14.5 and 16.5 mouse embryos, as well as neonatal mouse skin, using an anti-EPG antibody. Expression in the skin was observed in the hair follicles where EPG expression was detectable in relatively peripheral cells (Fig. 6*A*, *upper left panel*). Cross-sections of the follicle revealed that EPG expression was restricted to the inner and outer root sheath, a region of active proliferation, as detected by an anti-Ki67 antibody (Fig. 6*A*, *upper right panel*), whereas no expression was seen in the hair shaft. In embryos, EPG expression was detected in multiple developing structures. Two examples, the mouse tongue from an embryonic day 16.5 embryo (Fig. 6*A*, *lower left panel*) and the dorsal root ganglion from an embryonic day 14.5 embryo (Fig. 6*A*, *lower right panel*), are shown. In the developing tongue, EPG expression is largely localized to the papillae on the dorsal surface of the tongue and to the outer cell layers of the ventral surface (Fig. 6*A*, *lower left panel*, and data not shown). Likewise, high expression of EPG was observed in the dorsal root ganglion, where many members of the ErbB family ligands and receptors are expressed (29).

Next, we used the anti-EPG antibody to probe for EPG expression in human tissue microarrays of normal and invasive adenocarcinomas of the breast, as well as benign hyperplasia and adenocarcinomas of the prostate. EPG expression was observed in ductal epithelial cells of normal breast, and no expression was seen in benign hyperplasia of the prostate, as exemplified by staining of cross-sections of representative samples (Fig. 6*B*). However, EPG expression was observed in invasive adenocarcinomas of the breast and prostate. In both cases,

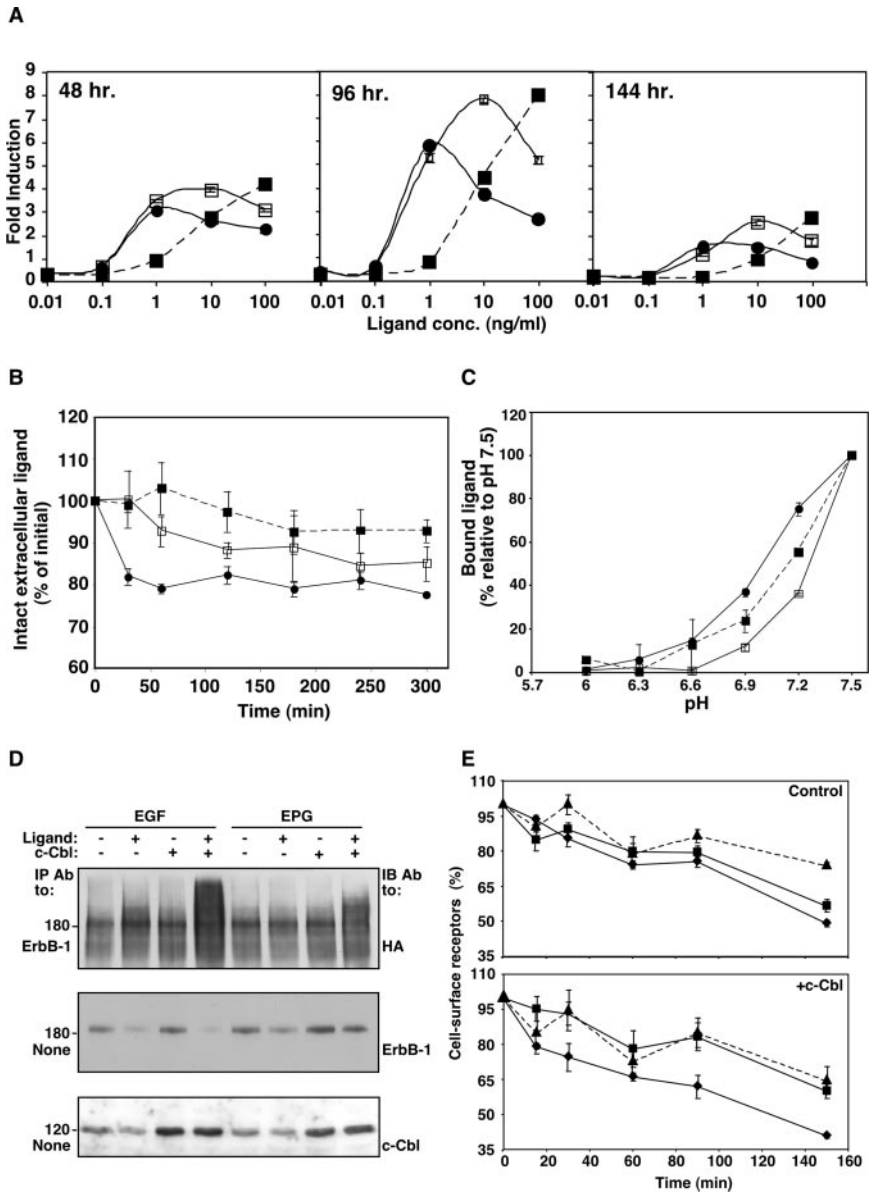

FIG. 5. **Ligand clearance and receptor degradation directly correlate with mitogenicity.** *A*, D1 cells were plated in triplicate in a 96-well plate and cultured in the presence of increasing concentrations (*conc.*) of EGF (*filled circles*), TGFα (*open squares*), or EPG (*filled squares* and *dashed line*) for the indicated period of time. A 3-(4,5-dimethylthiazol-2-yl)-2,5-diphenyltetrazolium bromide assay was performed at each time point. The values obtained are plotted as fold induction of cell proliferation with respect to the initial signal. *B*, Cos-7 cells were equally plated in 48-well plates and incubated with the following radiolabeled ligands (each at 10 ng/ml): EGF (*filled circles*), TGFα (*open squares*), and EPG (*filled squares* and *dashed lines*) for the indicated time intervals. At each time point, the acid-precipitable fraction of ligand in the medium and the cell surface-bound ligand was determined and the sum (mean ± range of duplicates) was plotted with respect to the initial amount of ligand added. *C*, the pH sensitivity of binding of radiolabeled EPG (*closed squares* and a *dashed line*), TGFα (*open squares*), and EGF (*diamonds*) was tested on A431 cells using phosphate solutions buffered at the indicated pH values (7.5–6.0). After 3 h of incubation on ice, the cells were washed, and cell-associated radioactivity was determined. The values (mean ± range of duplicates) are plotted with respect to ligand binding at pH 7.5. *D*, Cos-7 cells were transfected with plasmids encoding ErbB-1 and HA-tagged ubiquitin, along with either a control plasmid or a c-Cbl expression vector. Forty-eight hours later, the cells were stimulated for 10 min at 37 °C with EGF or EPG (each at 100 ng/ml), and whole cell extracts were analyzed using immunoblotting, either directly or after immunoprecipitation (*IP*). *E*, Cos-7 cells were transfected with plasmids encoding ErbB-1 and c-Cbl (*lower panel*) or ErbB-1 only (*upper panel*). Forty-eight hours later, the cells were treated at 37 °C with EGF (*diamonds*), TGFα (*filled squares*), or EPG (*filled triangles* and *dashed lines*; each at 100 ng/ml) for the indicated time intervals. At each time point, surface-bound ligand was stripped using ice-cold acidic solution, and the cells were incubated for 2 h with a radiolabeled EGF. The cells were later washed, and cell-associated radioactivity was determined. The value obtained for each time point (mean ± S.D.) was plotted with respect to the initial value. *Ab*, antibody.

expression was restricted to infiltrating epithelial cells, but no expression was observed in the adjoining stromal tissue, suggesting that EPG is an autocrine or an exocrine factor. We also isolated total RNA from prostate cancer xenografts grown in both castrated (androgen-independent) and noncastrated mice (androgen-dependent). Reverse transcriptase-PCR detected the expected 500-bp fragment in all but one of the xenografts tested (Fig. 6*C*), suggesting that EPG may be commonly expressed in prostate tumors but not necessarily in an androgen-dependent manner. In conclusion, expression in tumors, potent biological actions *in vitro*, and evasion of receptor inactivation indicate that EPG could be involved in oncogenesis.

Epigen Induces Biological Responses in Various Cell Types—Although ErbB-1 is the primary receptor for several EGF-like ligands, each growth factor appears to elicit specific biological responses. To compare the activity of EPG to other ErbB ligands, we used cell lines derived from tissues, in which EPG expression was detectable. EPG-treated MDA-MB-468 breast

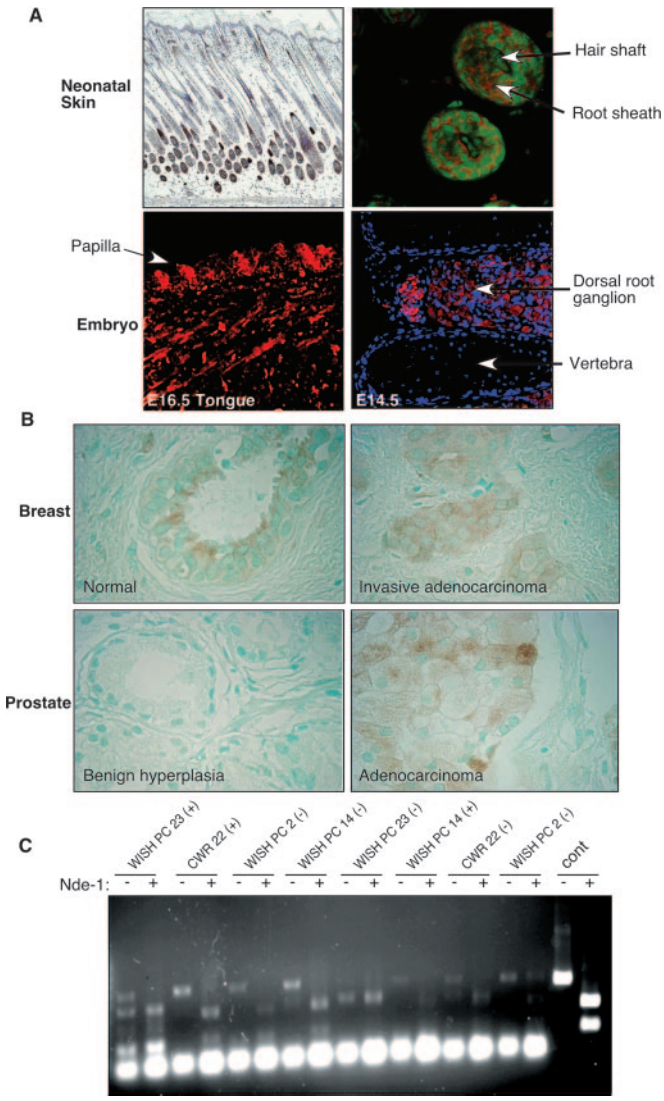

FIG. 6. **Epigen expression in normal mouse tissues and human tumors of the prostate and breast.** *A*, immunohistochemical analysis of EPG in the skin of a newborn (day 8) mouse (*upper panels*) and mouse embryos (*lower panels*). Anti-EPG (*red* or *brown*) and anti-Ki67 (*green*) antibodies were used and detection was performed using secondary fluorescent-labeled antibodies (*right panels*) or the Vectastain ABC system (*upper left panel*). Nuclei (*blue*) were detected by using Hoechst (Roche Applied Science). *B*, thin sections of paraffin-embedded normal human breast (*upper left panel*) and an invasive mammary adenocarcinoma (*upper right panel*) were stained with an affinity-purified rabbit anti-EPG antibody. Sections of paraffin-embedded benign human prostatic hyperplasia (*lower left panel*) and a prostate adenocarcinoma (Gleason score 7) were treated with an antibody to EPG (*lower right panel*) and processed as in *A*. Regions positive for EPG appear in *brown*. *C*, total RNA was extracted from prostate xenografts grown in normal (+) or castrated (−) athymic mice. PCR was performed using EPG-specific primers. A plasmid encoding the full-length *epigen* sequence was used as positive control (*cont.*). The PCR products were split into two, and one half was treated with NdeI to ensure that the product corresponds to *epigen*. WISH PC2 is an androgen-independent neuroendocrine small cell carcinoma (14), and CWR22 is an androgen-dependent adenocarcinoma.

carcinoma cells acquired a multifaceted phenotype that included flattened morphology, synthesis of milk proteins (casein) and neutral lipids, and enhanced expression of the intercellular adhesion molecule 1 (ICAM-1; Fig. 7*A* and data not shown). To assess the effect of EPG on the epithelium of the prostate, we used RWPE-1 normal prostate epithelial cells (17). When plated on growth factor-depleted Matrigel, these cells formed tubular structures with ascinar differentiation at the termini (Fig. 7*B*). Although TGFα and EPG caused the formation of ascini-like structures (Fig. 7*B*, *arrows*), ascini were not observed when these cells were stimulated with EGF. These differentiation-like effects of EPG and its expression in ganglia (Fig. 6*A*) prompted us to test the pheochromocytoma (PC12) model system, which has been extensively used to study neuronal differentiation. A PC12 derivative overexpressing ErbB-4 has previously been shown to respond to neuregulins in a manner indistinguishable from the response to neurotrophins (16). In comparison with untreated cells, PC12-ErbB-4 cells treated for 7 days with either NRG-1β, TGFα, or EPR developed neurite outgrowths and underwent enhanced proliferation in small colonies (Fig. 7*C* and data not shown). Although EPG elicited similar effects, the average length of neurite outgrowths was significantly shorter compared with NRG-1β-treated cultures.

ErbB receptors have been linked to angiogenesis as promoters of proliferation, as well as migration, of endothelial and vascular smooth muscle cells. To explore the possibility that EPG would function as a pro-angiogenic factor, we embedded mouse aorta rings in collagen as described (30), and treated them with different ligands for 10 days. EGF and EPG caused proliferation and migration of endothelial and smooth muscle cells, whereas the effect of NRG-1β was minor (Fig. 7*D* and data not shown). However, unlike vascular endothelial growth factor-treated rings, the migrating cells did not form microvessels, but a network of cells with long processes and limited cell-to-cell contacts (Fig. 7*D*). Taken together, the results presented in Fig. 7, as well as the observations made with 32D cells (Fig. 3), indicate that EPG induces both proliferation and differentiation of various target cell lineages.

DISCUSSION

The ErbB network of receptor tyrosine kinases has served as a rich source of lessons relevant to the mechanisms of signaling by growth factor receptors (reviewed in Ref. 7). Although it is clear that the mammalian ErbB network comprises four tyrosine kinases, the final number of their soluble ligands remains an open question, which reflects primarily on the mode of action of ErbB-2, the most oncogenic member of the family. Whether or not ErbB-2 can form homodimers in response to an EGF-like ligand has remained an elusive possibility, because no direct ligand of ErbB-2 has been identified. Along with the issue of an EGF-like ligand capable of directly stimulating ErbB-2, the present study addressed the functional significance of the occurrence of multiple ligands sharing ErbB-1 as a primary receptor. Based on genomic searches, we propose that the list of mammalian EGF-like ligands of ErbBs is already complete, such that no ligand with specificity to ErbB-2 might exist. On the other hand, the results obtained with EPG lead us to conclude that the family of EGF-like ligands may be divided into two groups; unlike high affinity ligands (*e.g.* EGF and HB-EGF), EPG, EPR, and Amphiregulin are low affinity ligands that gain high potency by evading physiological mechanisms of signaling desensitization.

Activity-based assays were used to detect and isolate ligands like TGFα, HB-EGF, and NRG-1. Other methods, including search algorithms based on mRNA sequence homology, were later used to identify yet other ligands like NRG-2 (31), NRG-3 (32), and NRG-4 (18). Because repeated screening of cDNA data bases failed to identify new ligands, we compared the genomic structures of EGF-like ligands and revealed a surprisingly conserved genomic organization (Fig. 1*A*). Algorithms based upon the common genomic structure and cDNA sequences reidentified all of the EGF-like ligands but failed to unravel novel molecules. Notably, however, the search we performed would be unable to detect inhibitory Argos-like ligands

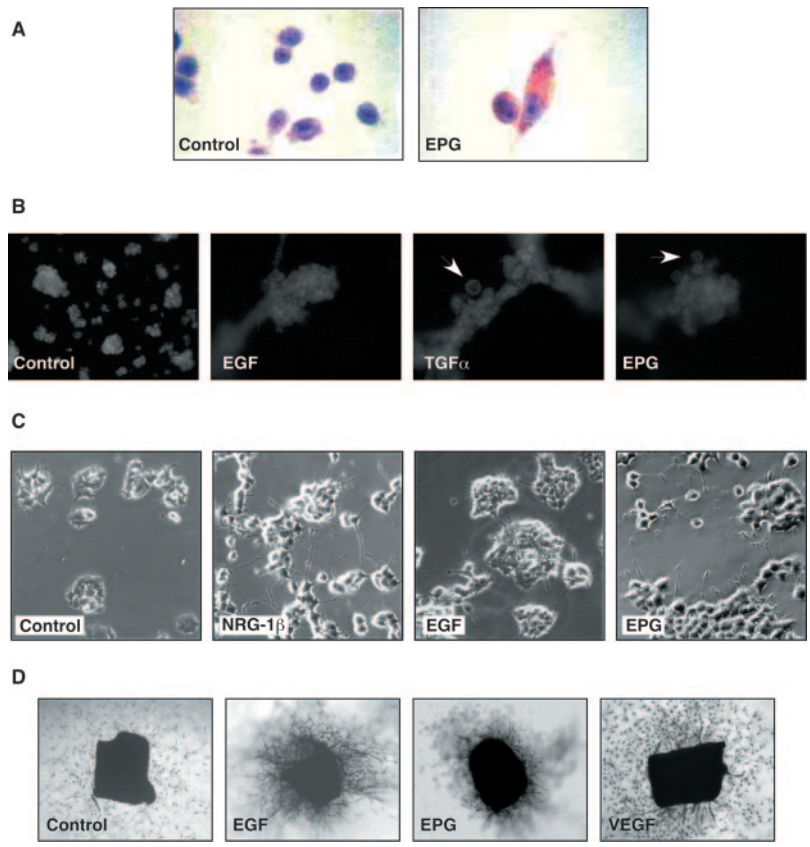

FIG. 7. **Epigen induces differentiation of mammary, prostate, pheochromocytoma and endothelial cells.** *A*, MDA-MB-468 human mammary carcinoma cells were incubated without or with EPG (100 ng/ml) for 4 days. The cells were then fixed and stained with Oil Red O (to visualize neutral lipids). *B*, human RWPE-1 prostate epithelial cells were plated on a layer of growth factor-depleted Matrigel (BD Bioscience, San Jose, CA) in the absence (*Control*) or presence of EGF, TGFα, and EPG (each at 100 ng/ml) and cultured for 5 days. The cells were then fixed and stained with 4′,6′-diamino-2-phenylindole to visualize nuclei. Micrographs were prepared using a fluorescence microscope (4× magnification). *C*, PC12 cells stably expressing ErbB-4 (PC12-ErbB-4) were plated in collagen-coated 24-well plates at 40% confluence and treated for 7 days with the indicated ligands (each at 100 ng/ml). Photomicrographs were taken using an inverted microscope (40× magnification). *D*, mouse aortic rings were embedded in collagen gels in the presence of the indicated growth factors (each at 100 ng/ml). Micrographs were taken following 10 days of culture at 37 °C using an inverted microscope (4× magnification).

of mammals, should they exist. Hence, with the exception of these caveats, it is conceivable that the search we designed is exhaustive, and by inference, no additional stimulatory ErbB ligands exist in the human and mouse genomes. If correct, the pattern of ligand-receptor pairing is extremely unbalanced; ErbB-1 and ErbB-4 each bind at least six ligands, ErbB-3 binds multiple alternatively spliced isoforms of two types of NRGs, but ErbB-2 has no assigned ligand.

What function is fulfilled by ErbB-2, if an orphan receptor scenario is to be abandoned? Several lines of evidence culminated with the contention that ErbB-2 acts as a ligand-less signaling subunit of ErbB-1, ErbB-3, and ErbB-4. Thus, ErbB-2 not only forms ligand-inducible heterodimers with ErbB-1 and other receptors, it is arguably the preferred partner of activated ErbBs (33, 34). The heterodimers formed are characterized by high ligand binding affinity and prolonged signaling (35, 36), which lead to enhancement of cellular responses to all ErbB ligands. Perhaps the most convincing support for the ligand-less contention emerged from the crystal structure of a truncated ErbB-2 extracellular domain (37, 38). The ligand-binding cleft of ErbB-1 is defined by two noncontiguous β-helical domains (25, 39), but the corresponding regions of ErbB-2 form an interface that would occlude a ligand (38). Moreover, unlike in ErbB-3 and ErbB-1, where the dimerization loop is released from intramolecular constraints only upon ligand binding, the respective loop of ErbB-2 is preactivated and poised to interact with other receptors (38). Therefore, a multitude of lines of evidence is consistent with the possibility that no unknown ErbB-2 ligands might exist, in line with the results of our genomic and cDNA searches.

The analyses presented in Fig. 1 suggest that all mammalian EGF-like ligands evolved from a single ancestor, which is represented by Vein in insects (Fig. 1*A*). Like in humans, multiple ligands exist in insects (reviewed in Ref. 40). However, the advantage of evolving several ligands with shared recognition is unclear. Genetic manipulations of mouse embryos imply that each ErbB ligand fulfills a unique function in embryonic and post-embryonic development. For example, both HB-EGF and Betacellulin bind ErbB-1, but mice defective for each factor display distinct phenotypes (41). Another example relates to mammary development, which seems to involve nonoverlapping activities of several ligands of ErbB-1 (42). In this respect, EPG displays unique features, including specificity to ErbB-1 (Figs. 3*C* and 4*C*), weak activation of ErbB-3 and ErbB-4 (Fig. 3, *E* and *F*), transient expression at the cell surface followed by two cleavage events (Fig. 2), and a variety of cellular activities that appear nonidentical to the effects elicited by other ligands of ErbB-1 (Fig. 7). Moreover, EPG expression is detectable in multiple organs of the mouse embryo, as well as under normal and pathological conditions of human tissues (Fig. 6).

The most remarkable feature of EPG is an apparent discrepancy between its relatively low receptor binding affinity (Fig. 4*C*) and a very potent mitogenic activity (Fig. 3, *C* and *D*). This raises the question of how a low affinity ligand gains mitogenic superiority. Our results indicate that EPG evades physiological mechanisms that normally desensitize growth factor signaling. Because these mechanisms depend on ligand-induced receptor activation, the low affinity binding of EPG translates into weak stimulation of the negatively acting mechanisms. For example, robust self-phosphorylation of ErbB-1 accompanies high affinity binding of EGF, but the weaker interaction with EPG results in faint receptor phosphorylation (Fig. 4, *A* and *B*) and reduced ability to recruit the c-Cbl ubiquitin ligase (Fig. 5*D*). Hence, the ubiquitylation-driven processes of receptor down-regulation (Fig. 5*E*) and lysosomal degradation (Fig. 5*D*) are defective in the case of EPG. Likewise, receptor-mediated endocytosis serves another function, namely rapid clearance of growth factors, but this process is relatively slow in the case of EPG (Fig. 5*B*). An additional feature that enhances Epigen's cellular effects is sensitivity of receptor binding to low pH (Fig.

5*C*), which is expected to enhance recycling of EPG, along with the internalized receptors (43). In summary, the anomalous potency of EPG is due to prolonged presence of the growth factor in the extracellular medium and ineffective receptor inactivation processes.

Our studies of EPG raise the possibility that the multiplicity of ligands sharing the same receptor reflects different relations between binding affinity, fate of ligand/receptor complexes, and distinct signaling patterns. A striking example is provided by a point mutant of EGF engineered for bioprocessing applications. This ligand is a more potent mitogenic stimulus than natural EGF, because its depletion from the medium of cells is relatively ineffective (22). Another example is provided by pathogenic viruses of the pox family, which invariably encode EGF-like growth factors that take advantage of the "low affinity/potent mitogenicity" principle (26). Likewise, EPR displays relatively low affinity, broad receptor specificity and anomalous potency (20, 44, 45). These considerations reinforce our proposition that EGF-like ligands may be categorized into high and low affinity growth factors. The two categories may differ in their mode of signaling; the high affinity factors (*e.g.* EGF, HB-EGF and NRG1-β) stimulate a robust but transient wave of response, whereas the low affinity ligands (*e.g.* EPG, EPR, and Amphiregulin) may elicit potent responses caused by ineffective metabolism of ligand-receptor complexes. Future studies will address the possibility that the physiological and pathological roles played by the low affinity category are distinct from the high affinity group. For example, the expression of several EGF-like ligands (*i.e.* Amphiregulin, EPR, TGFα, and HB-EGF) is coordinately up-regulated in androgen-independent prostate tumors (46). Whether or not EPG and other low affinity ligands play novel roles in human cancer will be the subject of our future studies.

Acknowledgments—We thank Drs. O. Brenner and O. Leitner for help with immunohistochemistry and antibody generation.

REFERENCES

1. Stein, R. A., and Staros, J. V. (2000) *J. Mol. Evol.* **50,** 397–412
2. Guy, P. M., Platko, J. V., Cantley, L. C., Cerione, R. A., and Carraway, K. L., III (1994) *Proc. Natl. Acad. Sci. U. S. A.* **91,** 8132–8136
3. Klapper, L. N., Glathe, S., Vaisman, N., Hynes, N. E., Andrews, G. C., Sela, M., and Yarden, Y. (1999) *Proc. Natl. Acad. Sci. U. S. A.* **96,** 4995–5000
4. Slamon, D. J., Godolphin, W., Jones, L. A., Holt, J. A., Wong, S. G., Keith, D. E., Levin, W. J., Stuart, S. G., Udove, J., Ullrich, A., and Press, M. F. (1989) *Science* **244,** 707–712
5. Salomon, D. S., Brandt, R., Ciardiello, F., and Normanno, N. (1995) *Crit. Rev. Oncol. Hematol.* **19,** 183–232
6. Baselga, J., Tripathy, D., Mendelsohn, J., Baughman, S., Benz, C. C., Dantis, L., Sklarin, N. T., Seidman, A. D., Hudis, C. A., Moore, J., Rosen, P. P., Twaddell, T., Henderson, I. C., and Norton, L. (1996) *J. Clin. Oncol.* **14,** 737–744
7. Yarden, Y., and Sliwkowski, M. X. (2001) *Nat. Rev. Mol. Cell. Biol.* **2,** 127–137
8. Riese, D. J., II, and Stern, D. F. (1998) *Bioessays* **20,** 41–48
9. Strachan, L., Murison, J. G., Prestidge, R. L., Sleeman, M. A., Watson, J. D., and Kumble, K. D. (2001) *J. Biol. Chem.* **276,** 18265–18271
10. Troyer, K. L., Luetteke, N. C., Saxon, M. L., Qiu, T. H., Xian, C. J., and Lee, D. C. (2001) *Gastroenterology* **121,** 68–78
11. Page, R. D. M. (1996) *Comput. Appl. Biosci.* **12,** 357–358
12. Hobbs, S., Jitrapakdee, S., and Wallace, J. C. (1998) *Biochem. Biophys. Res. Commun.* **252,** 368–372
13. Mosman, T. (1983) *J. Immunol. Methods* **65,** 55–63
14. Pinthus, J. H., Waks, T., Schindler, D. G., Harmelin, A., Said, J. W., Belldegrun, A., Ramon, J., and Eshhar, Z. (2000) *Cancer Res.* **60,** 6563–6567
15. Bacus, S. S., Gudkov, A. V., Zelnick, C. R., Chin, D., Stern, R., Stancovski, I., Peles, E., Ben Baruch, N., Farbstein, H., and Lupu, R. (1993) *Cancer Res.* **53,** 5251–5261
16. Vaskovsky, A., Lupowitz, Z., Erlich, S., and Pinkas-Kramarski, R. (2000) *J. Neurochem.* **74,** 979–987
17. Bello, D., Webber, M. M., Kleinman, H. K., Wartinger, D. D., and Rhim, J. S. (1997) *Carcinogenesis* **18,** 1215–1223
18. Harari, D., Tzahar, E., Romano, J., Shelly, M., Pierce, J. H., Andrews, G. C., and Yarden, Y. (1999) *Oncogene* **18,** 2681–2689
19. Pinkas-Kramarski, R., Soussan, L., Waterman, H., Levkowitz, G., Alroy, I., Klapper, L., Lavi, S., Seger, R., Ratzkin, B. J., Sela, M., and Yarden, Y. (1996) *EMBO J.* **15,** 2452–2467
20. Shelly, M., Pinkas-Kramarski, R., Guarino, B. C., Waterman, H., Wang, L. M., Lyass, L., Alimandi, M., Kuo, A., Bacus, S. S., Pierce, J. H., Andrews, G. C., and Yarden, Y. (1998) *J. Biol. Chem.* **273,** 10496–10505
21. Jones, J. T., Akita, R. W., and Sliwkowski, M. X. (1999) *FEBS Lett.* **447,** 227–231
22. Reddy, C. C., Niyogi, S. K., Wells, A., Wiley, H. S., and Lauffenburger, D. A. (1996) *Nat. Biotech.* **14,** 1696–1699
23. Wiley, H. S., and Burke, P. M. (2001) *Traffic* **2,** 12–18
24. Ebner, R., and Derynck, R. (1991) *Cell Regul.* **2,** 599–612
25. Garrett, T. P., McKern, N. M., Lou, M., Elleman, T. C., Adams, T. E., Lovrecz, G. O., Zhu, H. J., Walker, F., Frenkel, M. J., Hoyne, P. A., Jorissen, R. N., Nice, E. C., Burgess, A. W., and Ward, C. W. (2002) *Cell* **110,** 763–773
26. Tzahar, E., Moyer, J. D., Waterman, H., Barbacci, E. G., Bao, J., Levkowitz, G., Shelly, M., Strano, S., Pinkas-Kramarski, R., Pierce, J. H., Andrews, G. C., and Yarden, Y. (1998) *EMBO J.* **17,** 5948–5963
27. Thien, C. B., and Langdon, W. Y. (2001) *Nat. Rev. Mol. Cell. Biol.* **2,** 294–307
28. Levkowitz, G., Waterman, H., Zamir, E., Kam, Z., Oved, S., Langdon, W. Y., Beguinot, L., Geiger, B., and Yarden, Y. (1998) *Genes Dev.* **12,** 3663–3674
29. Buonanno, A., and Fischbach, G. D. (2001) *Curr. Opin. Neurobiol.* **11,** 287–296
30. Nicosia, R. F., and Ottinetti, A. (1990) *Lab. Invest.* **63,** 115–122
31. Chang, H., Riese, D. J., II, Gilbert, W., Stern, D. F., and McMahan, U. J. (1997) *Nature* **387,** 509–512
32. Zhang, D., Sliwkowski, M. X., Mark, M., Frantz, G., Akita, R., Sun, Y., Hillan, K., Crowley, C., Brush, J., and Godowski, P. J. (1997) *Proc. Natl. Acad. Sci. U. S. A.* **94,** 9562–9567
33. Graus Porta, D., Beerli, R. R., Daly, J. M., and Hynes, N. E. (1997) *EMBO J.* **16,** 1647–1655
34. Tzahar, E., Waterman, H., Chen, X., Levkowitz, G., Karunagaran, D., Lavi, S., Ratzkin, B. J., and Yarden, Y. (1996) *Mol. Cell. Biol.* **16,** 5276–5287
35. Beerli, R. R., Wels, W., and Hynes, N. E. (1994) *J. Biol. Chem.* **269,** 23931–23936
36. Karunagaran, D., Tzahar, E., Beerli, R. R., Chen, X., Graus Porta, D., Ratzkin, B. J., Seger, R., Hynes, N. E., and Yarden, Y. (1996) *EMBO J.* **15,** 254–264
37. Cho, H. S., Mason, K., Ramyar, K. X., Stanley, A. M., Gabelli, S. B., Denney, D. W., Jr., and Leahy, D. J. (2003) *Nature* **421,** 756–760
38. Garrett, T. P., McKern, N. M., Lou, M., Elleman, T. C., Adams, T. E., Lovrecz, G. O., Kofler, M., Jorissen, R. N., Nice, E. C., Burgess, A. W., and Ward, C. W. (2003) *Mol. Cell* **11,** 495–505
39. Ogiso, H., Ishitani, R., Nureki, O., Fukai, S., Yamanaka, M., Kim, J. H., Saito, K., Sakamoto, A., Inoue, M., Shirouzu, M., and Yokoyama, S. (2002) *Cell* **110,** 775–787
40. Shilo, B. Z. (2003) *Exp. Cell Res.* **284,** 140–149
41. Jackson, L. F., Qiu, T. H., Sunnarborg, S. W., Chang, A., Zhang, C., Patterson, C., and Lee, D. C. (2003) *EMBO J.* **22,** 2704–2716
42. Troyer, K. L., and Lee, D. C. (2001) *J. Mammary Gland Biol. Neoplasia* **6,** 7–21
43. Lenferink, A. E., Kramer, R. H., van Vugt, M. J., Konigswieser, M., Di Fiore, P. P., van Zoelen, E. J., and van de Poll, M. L. (1997) *Biochem. J.* **327,** 859–865
44. Toyoda, H., Komurasaki, T., Ikeda, Y., Yoshimoto, M., and Morimoto, S. (1995) *FEBS Lett.* **377,** 403–407
45. Riese, D. J., II, Komurasaki, T., Plowman, G. D., and Stern, D. F. (1998) *J. Biol. Chem.* **273,** 11288–11294
46. Torring, N., Jorgensen, P. E., Sorensen, B. S., and Nexo, E. (2000) *Anticancer Res.* **20,** 91–95